Supplementary Online Material for Mathematical Modelling of the Restenosis Process after Stent Implantation

Javier Escuer[1] · Miguel A. Martínez[1,2] · Sean McGinty[3] · Estefanía Peña[1,2]

This file includes:

- S1. Discussion related to Figures 9 and 10 of the sensitivity analysis
- S2. Supplemental figures related to the sensitivity analysis

S1 Discussion related to Figures 9 and 10 of the sensitivity analysis

A sensitivity analysis of the 28 parameters indicated in Table 1 of the main text was performed in order to evaluate the effect of varying each input parameter involved on the evolution of the restenosis process and to test the robustness of the results of the computational model. This is of particular importance because of the absence of a complete set of experimental data and the variability seen in many of the parameters. However, only those parameters whose variation showed the greatest impact on the results have been included in the main text. The discussion corresponding to those figures is detailed in this section.

Local variations of GFs, MMPs, ECM and SMCs at point A, located close to a central stent strut in the media, are illustrated in Fig. 10 for 8 different cases. The results shown for point B correspond exclusively to the baseline model. The variables of the system damage, d, and local density of endothelial cells, c_{ec}, do not experience large changes with the variation of the parameters, so the results corresponding to these variables have not been included in this work.

The damage degradation rate, $k_{deg,d}$, is an estimated parameter from experimental data directly proportional to the healing rate of the tissue. As can be seen in Fig. 9 of the main text, for high values of $k_{deg,d}$, the level of damage in the arterial wall decreases more rapidly and consequently the healing process is accelerated. The reference value for this parameter has been calibrated according to experimental data that shows that the damage caused by the device implantation is restored after approximately 300 days. The

[1]Applied Mechanics and Bioengineering Group (AMB), Aragón Institute of Engineering Research (I3A), University of Zaragoza, Zaragoza, Spain.
[2]Biomedical Research Networking Center in Bioengineering, Biomaterials and Nanomedicine (CIBER-BBN), Spain.
[3]Division of Biomedical Engineering, University of Glasgow, Glasgow, UK.

impact of this parameter on the evolution of the biological species is studied in Case 01. When $k_{deg,d}$ is decreased, we observe an increase in the local maximum concentrations of GFs, MMPs and of the local densities of SMC and a slowing down of the temporal response of these species, representing a longer time to reach their maximum and the final equilibrium. However, reduced equilibrium concentrations are shown for the ECM components when $k_{deg,d}$ decreases. It is important to highlight that when the healing process is faster ($k_{deg,d}$ higher), the concentration levels of ECM components in the tissue are also higher, and this ultimately leads to an increased tissue growth.

When $k_{prod,gf}$ is varied, Case 02, a general rise in the local concentrations and densities of all the species is observed when the value of this parameter is increased. Furthermore, we observe a reduction in the initial degradation of the ECM and in the differentiation of the contractile SMCs into the synthetic phenotype with increasing values of this parameter. Therefore, the increase observed in the local density of synthetic SMCs with $k_{prod,gf}$ is mainly due to their proliferation by the action of GFs. Similar behaviour of the system is observed when the impact of the synthetic SMCs proliferation rate by the GFs, $k_{prolif,ssmc}$ (Case 11) is analysed. A very similar response can also be obtained by varying the initial concentration of MMP, $c_{mmp,0}$, in Case 19. It should be noted that in this case the normalized local concentrations and densities, $c_j/c_{j,0}$, were represented in order to establish comparisons with the other cases simulated.

On the one hand, when the MMP production rate by the contractile SMCs, $k_{prod1,mmp}$, is modified in Case 05, an increase in the local concentration of MMPs and in the local density of synthetic SMC is observed at point A when the parameter value rises. Moreover, the instant in which the peaks appear in their time-varying profiles is independent of the value for these species. On the other hand, the local concentration of GFs, ECM and the local density of contractile SMC at point A is reduced if the value of $k_{prod1,mmp}$ increases. Furthermore, an increase in the initial degradation of the ECM and in the differentiation of the contractile SMC into the synthetic phenotype, can be noted when the value of this parameter increases, resulting in lower restenotic growth at the end of the simulation. Similar responses are observed when the ECM degradation rate, $k_{deg,ecm}$ (Case 08) is varied.

In Case 10, small changes are observed in the temporal response of GFs and MMPs when varying the differentiation rate from synthetic to contractile SMCs, $k_{diff,ssmc}$, is analysed. However, for the rest of the species considered, the changes are notable. In general, local concentrations and densities of ECM and SMCs increase when the value of this parameter decreases. However, the variation of $k_{diff,ssmc}$ does not affect the level of the initial degradation of the ECM or the amount of contractile SMCs differentiated into synthetic phenotype. In case of synthetic SMCs, when $k_{diff,ssmc}$ increases a slower response is observed in the time-varying local density profiles, meaning that they take longer to revert to the contractile phenotype.

In general, the variation of the diffusion coefficients does not generate relevant changes in the time-varying profiles for most of the species. In Case 15, as a representative example of the effect of varying the diffusivity, the influence of the variation of the MMP diffusion coefficient, D_{mmp}, is shown. It can be noted that D_{mmp} has virtually no effect on GFs and synthetic SMCs and only slightly affects the local concentrations of MMPs and ECM components. However, a decrease in the density of contractile SMCs at point A is observed when the MMP diffusivity decreases.

We note the appearance of possible numerical instabilities when observing the time-varying concentration profiles of ECM, which is the substance most sensitive to changes

in many of the parameters. This is primarily due to numerical issues caused by the reduction of the shape function order used in the discretization of the FE mesh only in the sensitivity analysis, in order to achieve faster computational times. However, these issues do not affect the global behaviour of the system and the general conclusions of this section.

S2 Suplemental figures related to the sensitivity analysis

Here, the results for the rest of the cases simulated are shown.

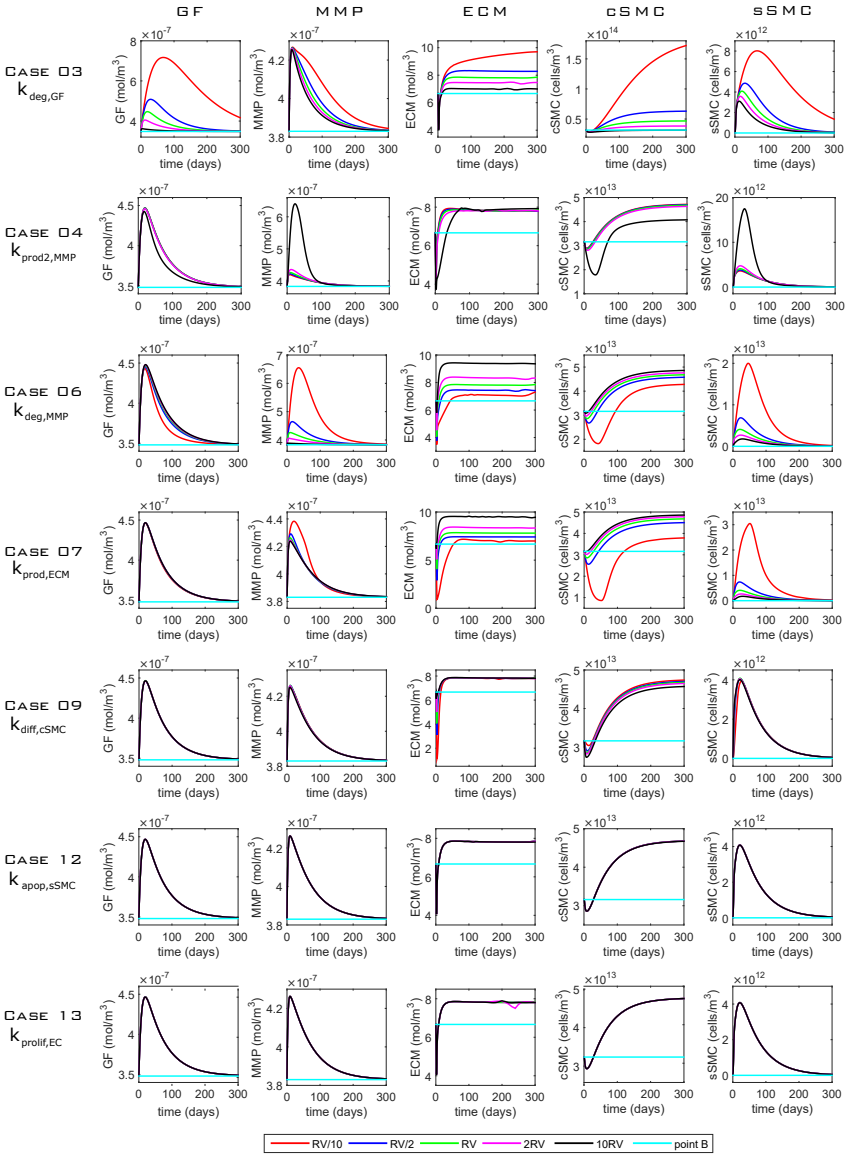

Fig. S1: Supplemental results from the sensitivity analysis related to the rates. The plots show the effect of varying several rates on the concentration of GFs, MMPs and ECM as well as the density of contractile and synthetic SMCs. Computations were carried out for four different values for each parameter apart from the reference value, RV, which is shown in Table 2 of the main text. The values of 2RV and RV/2 were considered $\pm$ half the RV of the selected parameter; 10RV and RV/10 were given by increasing and decreasing by one order of magnitude the RV (see Table 3 of the main text). The results shown for point B correspond exclusively to the RV (baseline model).

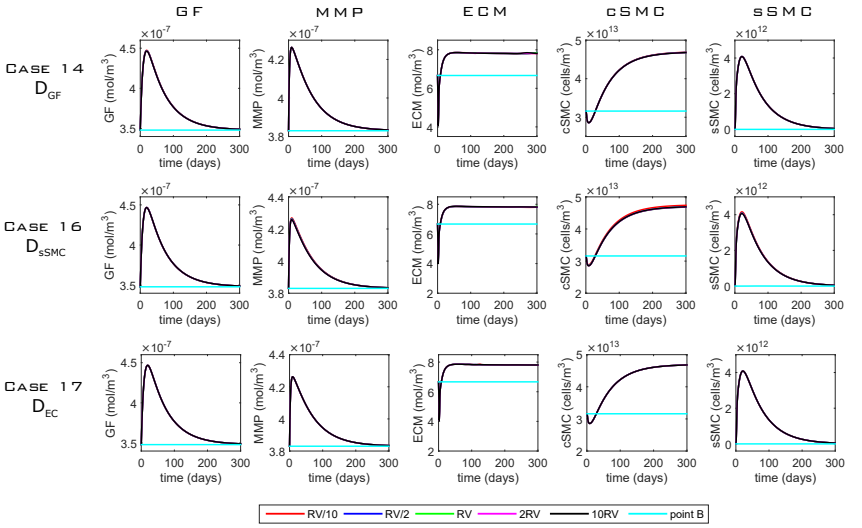

Fig. S2: Supplemental results from the sensitivity analysis related to the diffusion coefficients. The plots show the effect of varying several diffusivities on the concentration of GFs, MMPs and ECM as well as the density of contractile and synthetic SMCs. Computations were carried out for four different values for each parameter apart from the reference value, RV, which is shown in Table 2 of the main text. The values of 2RV and RV/2 were considered $\pm$ half the RV of the selected parameter; 10RV and RV/10 were given by increasing and decreasing by one order of magnitude the RV (see Table 3 of the main text). The results shown for point B correspond exclusively to the RV (baseline model).

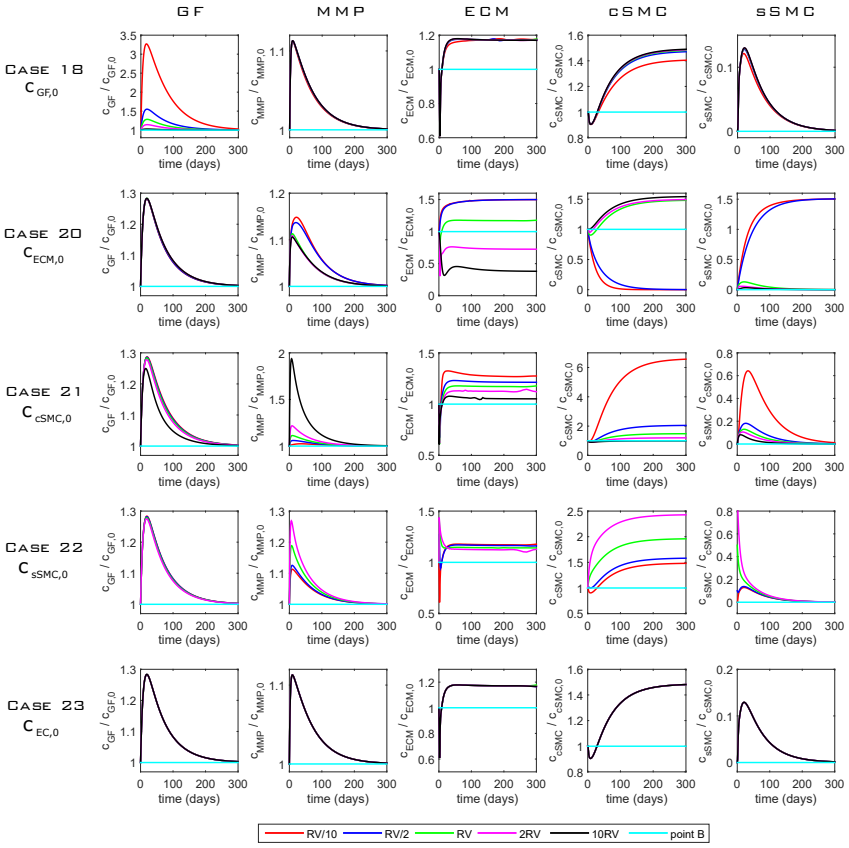

Fig. S3: Supplemental results from the sensitivity analysis related to the initial concentrations. The plots show the effect of varying several initial conentrations on the concentration of GFs, MMPs and ECM as well as the density of contractile and synthetic SMCs. Computations were carried out for four different values for each parameter apart from the reference value, RV, which is shown in Table 2 of the main text. The values of 2RV and RV/2 were considered $\pm$ half the RV of the selected parameter; 10RV and RV/10 were given by increasing and decreasing by one order of magnitude the RV (see Table 3 of the main text). The results shown for point B correspond exclusively to the RV (baseline model).

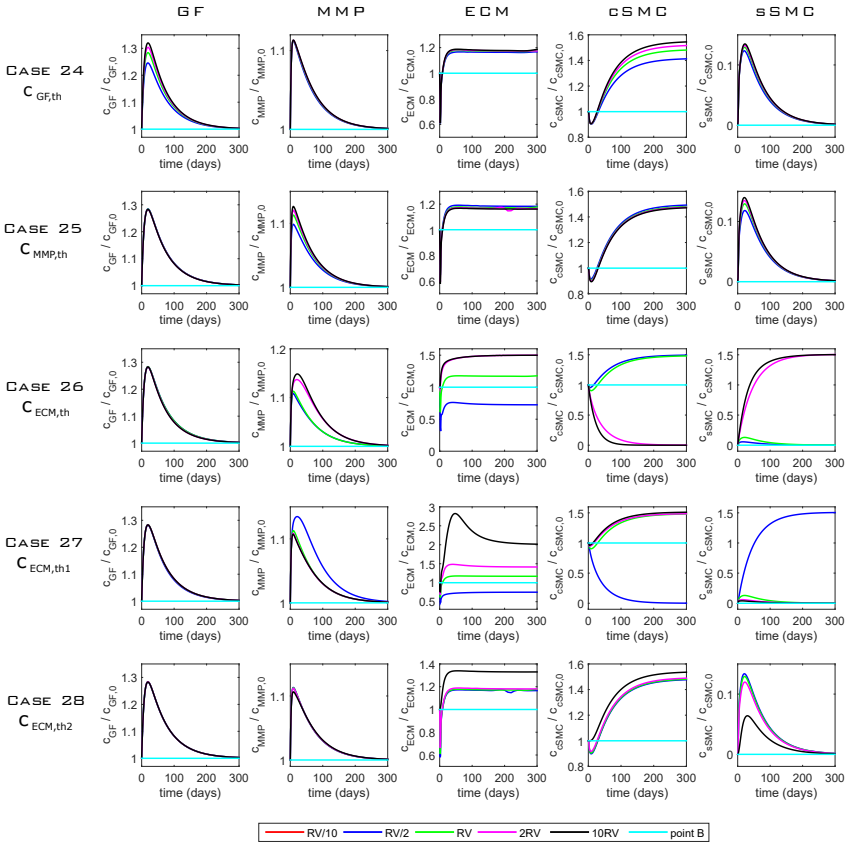

Fig. S4: Supplemental results from the sensitivity analysis related to the threshold values. The plots show the effect of varying the threshold values on the concentration of GFs, MMPs and ECM as well as the density of contractile and synthetic SMCs. Computations were carried out for four different values for each parameter apart from the reference value, RV, which is shown in Table 2 of the main text. The values of 2RV and RV/2 were considered $\pm$ half the RV of the selected parameter; 10RV and RV/10 were given by increasing and decreasing by one order of magnitude the RV (see Table 3 of the main text). The results shown for point B correspond exclusively to the RV (baseline model).